

Dynamics of nano tippe top

Yue Chan*, Ngamta Thamwattana and James M. Hill

Nanomechanics Group, School of Mathematics and Applied Statistics,
University of Wollongong, Wollongong, NSW 2522, Australia

February 12, 2022

Abstract

We investigate the motion of a nano tippe top, which is formed from a C_{60} fullerene, and which is assumed to be spinning on either a graphene sheet or the interior of a single-walled carbon nanotube. We assume no specific geometric configuration for the top, however for example, the nano tippe top might be formed by joining a fullerene C_{60} with a small segment of a smaller radius carbon nanotube. We assume that it is spinning on a graphene sheet or a carbon nanotube surface only as a means of positioning and isolating the device, and the only effect of the graphene or the carbon nanotube surface is only through the frictional effect generated at the point of the contact. We employ the same basic physical ideas originating from the classical tippe top and find that the total retarding force, which comprises both a frictional force and a magnetic force at the contact point between the C_{60} fullerene and the graphene sheet or the inner surface of the single-walled carbon nanotube, induces the C_{60} molecule to spin and precess from a standing up position to a lying down position. Unlike the classical tippe top, the nanoscale tippe top does not flip over since the gravitational effect is not sufficient at the nano scale. After the precession, while the molecular top spins about its lying down axis, if we apply the opposite retarding magnetic force at the contact point, then the molecule will return to its standing up position. The standing up and the lying down configurations of the nano tippe top during the precession and retraction processes demonstrate its potential use as a memory device in nano-computing.

1 Introduction

The discovery of fullerenes [1] and carbon nanotubes [2] has led to numerous studies on their properties and their various potential applications in nano devices. In this paper, we focus on the mechanics of a nanoscale tippe top comprising a fullerene C_{60} which for example might be joined to a carbon nanotube and is spinning on a graphene sheet or inside a large single-walled carbon nanotube. We assume that the nano tippe top is at the equilibrium configuration either on the graphene sheet or inside the outer carbon nanotube and that the spinning occurs due to the application of an external magnetic

*Corresponding author's email address: yc321@uow.edu.au

field. We refer to this structure as a nano tippe top or simply as a nano top. We note that in the case of the top spinning inside a nanotube, that although the effect of the outer carbon nanotube is not directly incorporated into our calculations, we have in mind that the outer carbon nanotube acts as a barrier between the nano top and the external environment.

The flip over of the classical tippe top has attracted much attention due to its “apparent” violation of the principle of conservation of energy during the top’s inversion (i.e. the rise in its center of mass results in the sudden increase in its potential energy but apparently no gain in other energies) as well as the lack of a complete mathematical description of this inversion phenomenon [3, 4, 5, 6, 7, 8, 9]. However, Cohen [10] provides an analysis and a numerical study on the tippe top. He views the tippe top as an eccentric sphere, for which its center of mass is different from its geometric center, and incorporates into his model Coulomb friction at the contact point to describe the tippe top’s motion. For example, this eccentric sphere can be manufactured either by creating the top with two different mass densities or by puncturing the sphere and inserting a stem. At the nano scale, the latter method may be achieved by introducing a defect on the surface of a fullerene C_{60} and then joining to this defect a small segment of a carbon nanotube. We refer the reader to Nasibulin *et al.* [11] for the possible creation of such nano tippe tops. Classically, the friction between the eccentric sphere and the relatively rough surface plays a vital role for the top’s inversion, and the sudden gain in the potential energy during the inversion results from the loss in the top’s rotational kinetic energy, which can also be observed from the reduction in the spinning of the inverted top. Furthermore, since gravity and the normal force act solely along the axis fixed in space and provide zero torque to the top, the friction, which acts offset from the space-fixed axis and against the rotational motion of the top, and is therefore the only source providing an external torque to slow the spinning of the top down [8]. In addition, Ueda *et al.* [13] show theoretically that the top’s initial spinning and the ratio of the top’s two different principal moments of inertia at the center of mass play an important role to determine the top’s inversion. For example, the flip over phenomenon can only occur when its initial spinning is above a certain threshold. Since friction at the nano scale is ultra-low [14, 15], our numerical results show that the friction itself is insufficient to make the nano tippe top precessing about the fixed-body axis. Therefore, in this paper we introduce a sufficiently large retarding magnetic force at the contact point to act analogously to the effect of friction. However, we find numerically that instead of flipping over, the nano top prefers to spin in a stable lying down configuration, which suggests that the effect of gravity is negligible at the nano scale. In particular, the nano top behaves more like a hard-boiled egg spinning on a rough surface [16].

As mentioned above, to induce the spinning effect of a nano top we introduce a retarding magnetic force at the contact point between the fullerene C_{60} and the carbon nanotube’s wall. We find from Wood *et al.* [17] who experimentally produce ferromagnetic fullerenes C_{60} that the magnetically strongest fullerenes are formed at 800 K with the magnetic moment per molecule of $0.38\mu_B$, where μ_B denotes the Bohr magneton constant. This result indicates that we can initiate the spinning of a fullerene in a preferred direction by applying an external magnetic field to the center of the fullerene and similarly at the contact point for generating the retarding magnetic force.

In the following section, we briefly state vector equations which are used to describe motion of a tippe top. We note that explicit forms of these equations are given in Appendix

A. In Section III, we provide numerical results for a nano tippe top, which is driven by a constant magnetic force in both x - and y -directions. We verify our numerical schemes by examining the classical tippe top, as presented in Appendix A. Conclusion of the paper is given in Section IV. In Appendix B, we use the basic equations as given in Appendix A to study the stability for certain configurations of a nano tippe top and in particular Appendix C considers the compatibility between our numerical results and asymptotic expansions when the nano top is in the lying position. Finally, while Section III considers $H_x = H_y = H$, in Appendix D we assume a magnetic force which is applied only in the y -direction and only for a finite time t_0 .

2 Equations of motion

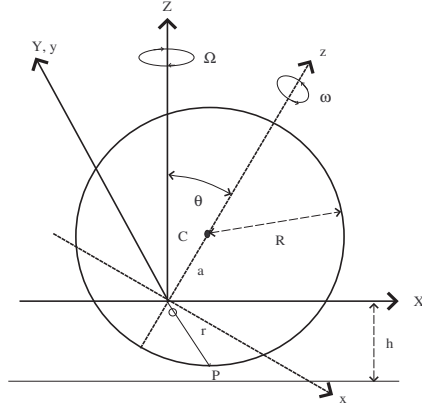


Figure 1: Schematic of nano tippe top

In this section, we state the equations of motion for a nano tippe top, which is schematically illustrated in Fig. 1. Owing to the axially symmetry of the density of the nano top and its eccentric structure, we assume that the center of mass O is at a distance a away from its geometric center C . We denote coordinates (X, Y, Z) as the space-fixed frame of the top while (x, y, z) as the body-fixed frame. We adopt (ϕ, θ, ψ) as the usual Euler angles relative to the space-fixed frame so that $\Omega = \dot{\phi}$. In addition, we choose the axes OY and Oy such that they coincide for all time. Therefore, the space-fixed frame and the body-fixed frame are different only through the rotation of the nutation angle θ . Furthermore, we suppose that the spinning about the space-fixed frame is $\mathbf{\Omega}(t) = (0, 0, \Omega)$ and the spinning about the body-fixed frame as ω where Ω denotes angular frequency about the Z -axis, and the nano top is assumed to be initially spinning about the axis Oz with an angular frequency ω . The distance between the surface and the center of mass is $h(\theta) = R - a \cos \theta$ and the position vector OP is $\mathbf{r} = (a \sin \theta, 0, -h(\theta))$. From the above quantities, the total angular velocity \mathbf{n} and the total angular momentum \mathbf{L} of the nano tippe top's system in the body-fixed frame are given respectively by

$$\begin{aligned} \mathbf{n} &= ((\omega - \Omega \cos \theta) \sin \theta, \dot{\theta}, \Omega \sin^2 \theta + \omega \cos \theta), \\ \mathbf{L} &= ((C\omega - A\Omega \cos \theta) \sin \theta, A\dot{\theta}, A\Omega \sin^2 \theta + C\omega \cos \theta), \end{aligned} \tag{1}$$

where (A, A, C) denote the principal moments of inertia at the center of mass O . In addition, the translational velocity at the contact point P with respect to O can be written as $\mathbf{v}_{r_P} = \mathbf{n} \times \mathbf{r}$ and hence the sliding velocity at P is given by $\mathbf{v}_p = \dot{\mathbf{X}} + \mathbf{v}_{r_P}$, where $\dot{\mathbf{X}} = (u_x, u_y, u_z)$ denotes the velocity of the center of mass of the nano top. The equations of motion of the nano top can then be determined for the six degrees of freedom motion comprising three rotational equations derived from the Euler equations and three translational equations derived from Newton second law, namely

$$\begin{aligned} \frac{\partial \mathbf{L}}{\partial t} + \mathbf{\Omega} \times \mathbf{L} &= \mathbf{r} \times (\mathbf{N} + \mathbf{F}), \\ m(\ddot{\mathbf{X}} + \mathbf{\Omega} \times \dot{\mathbf{X}}) &= \mathbf{N} + \mathbf{F} + \mathbf{W}, \end{aligned} \quad (2)$$

where m , \mathbf{N} , \mathbf{F} , \mathbf{W} denote the mass, the normal force, the retarding force and the weight of the nano top, respectively. Explicit forms of these equations of motion are given in Appendix A of Ueda *et al.* [13] and they are also briefly stated in the appendix of this paper. Next, we determine a suitable form of the frictional force for the proposed nano tippe top system. Various theoretical [18, 19] and molecular dynamics studies [20, 21] suggest that under the low velocity limit, the frictional force between two molecules is linearly proportional to their relative velocity. In addition, Heo *et al.* [22] propose that the frictional force between a fullerene and a carbon nanotube is also proportional to the fullerene's normal reaction, namely $|\mathbf{F}_f| = \mu N$. Further, molecular dynamics simulations of Heo *et al.* [22] show that the frictional coefficients for various nanostructures, namely single-walled carbon nanotubes, nanopeapods and double walled carbon nanotubes, under a low pressure regime, are essentially the same, i.e. $\mu = 0.13$. In this paper, we also incorporate a retarding magnetic force to the model and we propose that the total retarding force of the nano top inside the carbon nanotube is given by

$$\mathbf{F} = -\mathbf{F}_f - \mathbf{H}(B) = -\frac{0.13N}{|\mathbf{v}_P|} \mathbf{v}_P - \mathbf{H}(B), \quad (3)$$

where $\mathbf{H}(B)$ denotes the retarding magnetic force acting at P and \mathbf{v}_P is the velocity at the contact point P .

3 Numerical results and discussion

A fourth order Runge-Kutta method [23] is adopted here to numerically solve this system of six ordinary differential equations, namely Eq. (2). Ueda *et al.* [13] show that in macro scale the top's inversion is strongly dependent on the ratio of two principal moments of inertia at the center of mass. Therefore, we check whether the inversion of the nano top is possible by running the numerical scheme with various values of $C/A \in (0, 1)$, but we find that this ratio does not effect our numerical results. However, in all cases a sufficiently large initial spinning of the nano top is required. Therefore, we choose the following physical parameters for the numerical iteration: $R = 3.55 \text{ \AA}$, $a = 0.1R$, $m = 1.196 \times 10^{-24} \text{ kg}$, $A = (2/3)mR^2$, $C = 0.5A$ and $H_x = H_y = 0.1 \text{ zN}$ with the following initial conditions: $\theta = 0.1$, $\Omega = 0$, $\dot{\theta} = 0$, $\omega = 100$ and $\dot{\mathbf{X}} = (0, 0, 0)$. These initial conditions can be interpreted that we release the nano top with its initially spinning (100 Hz) about the z -axis, having 0.1 rad deflection from the Z -axis and zero sliding velocity at the contact point P . We use 500 grid points to carry out the numerical iteration and the numerical results obtained for θ , Ω and ω are illustrated in Figs. 2, 3 and 4, respectively.

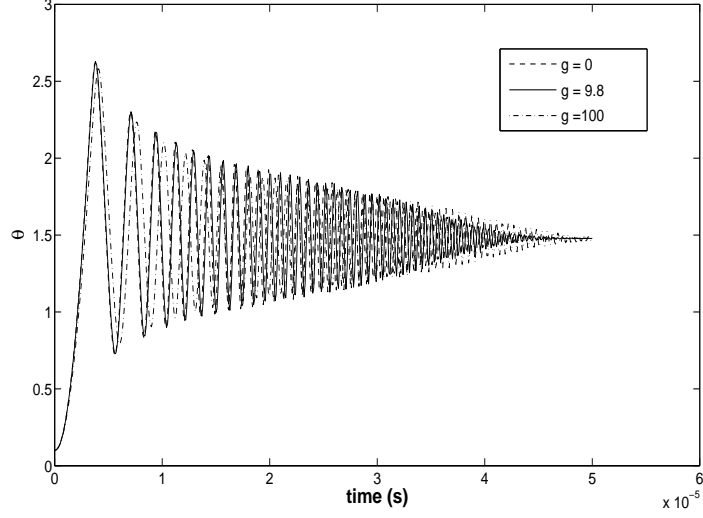


Figure 2: Nutation angle θ for $g = 0, 9.8$ and 100 ms^{-2} during precession

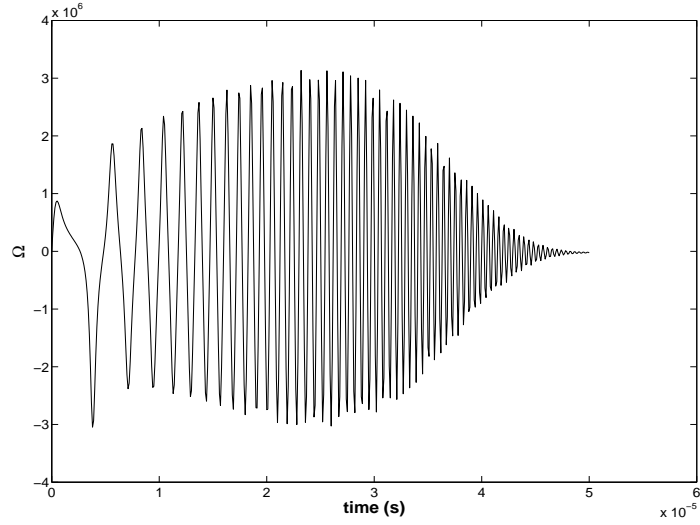


Figure 3: Angular frequency Ω about the Z -axis during precession

Under the total retarding force, which comprises both the frictional and the magnetic forces at the point of contact P , Fig. 2 shows that the nano top precesses from its standing up configuration ($\theta = 0$) during the first $5 \mu\text{s}$ but asymptotically approaches the lying down configuration ($\theta = \pi/2$) after $50 \mu\text{s}$ with the decrease in its oscillating amplitude. During the precession, as shown in Fig. 3, the angular frequency Ω about the Z -axis increases dramatically in the first micro second indicating the sudden drop down of the nano top but oscillating around zero while the nano top has laid down. On the other hand, from Fig. 4 the angular frequency ω about the z -axis also drops from its initial positive value to zero and then monotonically increases in magnitude to 30 MHz but in the opposite direction with respect to the direction of the initial spinning. This implies

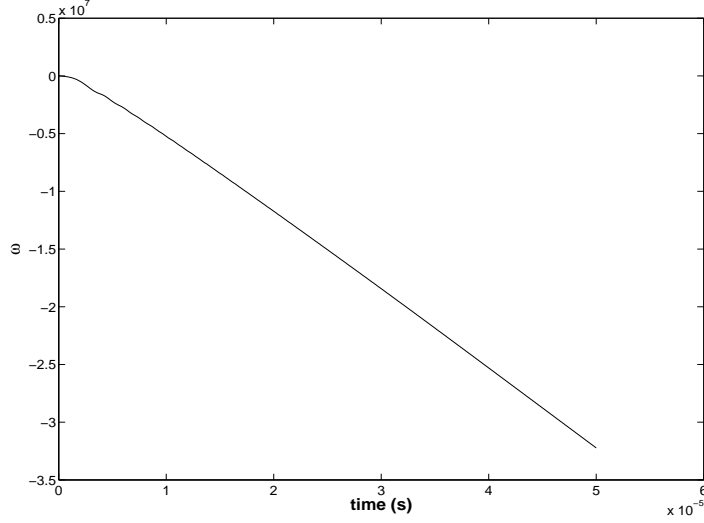


Figure 4: Angular frequency ω about the z -axis during precession

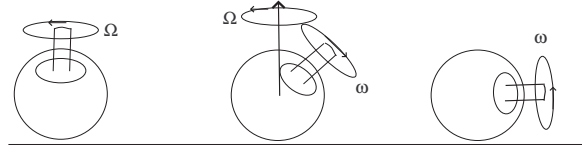


Figure 5: Precession of nano tippe top

that the nano top reverses its spinning direction and gains its spinning speed due to the opposite motion and the energy gained from the retarding magnetic force respectively. We also note that the center of mass of the nano top moves in the X, Y -directions only resulting in sliding friction but remains intact in the Z -direction (see Figs. 10 and 11). The whole precession process is illustrated in Fig. 5. Unlike the classical tippe top, we observe no flip over phenomenon in the nano top's precession. This no inversion phenomenon arises from the fact that the gravitational force is negligibly small at the nano scale. As confirmed by Fig. 2, the precession is not effected by the gravitational force since the numerical results for $g = 0$ and 9.8 ms^{-2} almost coincide with each other, and the same behaviour is obtained for $g = 100 \text{ ms}^{-2}$.

Once the nano top is spinning about the lying down axis, it is important to determine a possible way for which the nano top can retract to its initial standing up position. We find that the nano top will retract smoothly back to its standing up axis upon applying a magnetic force of the same magnitude but in the opposite direction to the previous retarding magnetic force and the numerical solution for θ is shown in Fig. 6.

Accordingly, by adjusting the magnetic field, we can manually control the nano top's switching between the standing up and the lying down states and hence it can be utilized as a nano-computing memory device. Moreover, the main advantages of utilizing the nano tops as a memory device are that it possesses a remarkably short relaxation time ($\approx 50 \mu\text{s}$) resulting in a higher computational speed, and it is small in size and hence provides a larger memory capacitance. Most importantly, it is simpler to control as compared with

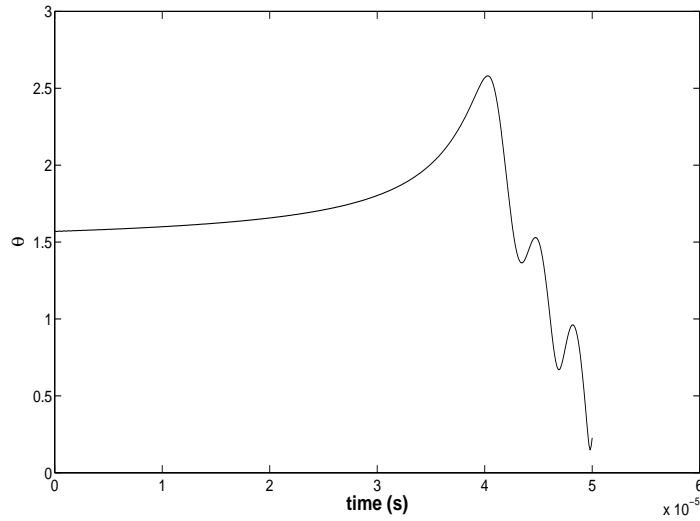


Figure 6: Nutation angle θ after applying the reversed retarding magnetic field at P

the electron-spin quantum memories. Finally, the integration of the self-assembled hybrid nanostructure known as nanopeapods and the ideas of nano tippe top developed here may lead to practical computing memory devices, which currently require large numbers of bit handling.

4 Conclusion

A nano tippe top formed from a C_{60} fullerene and spinning either on a graphene sheet or inside a carbon nanotube is investigated as a possible candidate for a computing memory device. The equations of motion for such a nano top are described and we find that while the retarding magnetic force makes the nano top precess, it does not flip over as in the classical tippe top, but due to the fact that gravity is negligible at the nano scale, it adopts a lying down position. In addition, while the nano top is in the lying down position, if we apply the magnetic force which is of the same magnitude but in the opposite direction to the previous retarding magnetic force, then the nano top will return to its standing up position. Hence, the standing up and lying down configurations of the nano top might be considered as two bit states, which gives rise to their potential use as a future memory device.

Acknowledgements

The authors are grateful for the Australian Research Council for support through the Discovery Project Scheme and the provision of an Australian Postdoctoral Fellowship for NT and an Australian Professorial Fellowship for JMH.

A Equations of motion

Here, we briefly state explicit forms of equations of motion obtained from Eq. (2). From Eq. (2)₁, the three rotational equations are given by

$$\begin{aligned} A\ddot{\theta} &= -\Omega(C\omega - A\Omega \cos \theta) \sin \theta - aN \sin \theta - h(\theta)F_x, \\ A \sin \theta \dot{\Omega} &= (C\omega - 2A\Omega \cos \theta)\dot{\theta} + (a - R \cos \theta)F_y, \\ C\dot{\omega} &= R \sin \theta F_y, \end{aligned} \quad (4)$$

where $h(\theta) = R - a \cos \theta$. From Eq. (2)₂ the three translational equations are of the form

$$\begin{aligned} m\dot{u}_x &= m\Omega u_y + F_x, \\ m\dot{u}_y &= -m\Omega u_x + F_y, \\ m\dot{u}_z &= N - mg, \end{aligned} \quad (5)$$

where

$$\begin{aligned} F_x &= \frac{-\mu N \{u_x - h(\theta)\dot{\theta}\}}{\sqrt{\{u_x - h(\theta)\dot{\theta}\}^2 + \{u_y + [R(\omega - \Omega \cos \theta) + a\Omega] \sin \theta\}^2}} \\ &\quad - H_x, \\ F_y &= \frac{-\mu N \{u_y + [R(\omega - \Omega \cos \theta) + a\Omega] \sin \theta\}}{\sqrt{\{u_x - h(\theta)\dot{\theta}\}^2 + \{u_y + [R(\omega - \Omega \cos \theta) + a\Omega] \sin \theta\}^2}} \\ &\quad - H_y, \end{aligned} \quad (6)$$

and H_x and H_y denote the strength of the retarding magnetic force in the x - and y -directions respectively. By multiplying $\sin \theta$ both sides of Eq. (4)₂ we obtain

$$A \sin^2 \theta \dot{\Omega} = (C\omega - 2A\Omega \cos \theta) \sin \theta \dot{\theta} + (a - R \cos \theta) F_y \sin \theta. \quad (7)$$

From Eq. (4)₃ we have $F_y \sin \theta = C\dot{\omega}/R$, which upon substituting into Eq. (7) we have

$$A \sin^2 \theta \dot{\Omega} + 2A\Omega \cos \theta \sin \theta \dot{\theta} = C\omega \sin \theta \dot{\theta} - C\dot{\omega} \cos \theta + aC\dot{\omega}/R,$$

which can be written as

$$A \frac{d(\Omega \sin^2 \theta)}{dt} = \frac{aC}{R} \frac{d\omega}{dt} - C \frac{d(\omega \cos \theta)}{dt}. \quad (8)$$

Thus, from Eq. (8) we obtain

$$A\Omega \sin^2 \theta = aC\omega/R - C\omega \cos \theta + J^*, \quad (9)$$

where J^* is a constant of integration. By multiplying R both sides of Eq. (9) we have

$$J = A\Omega R \sin^2 \theta + C\omega(R \cos \theta - a), \quad (10)$$

where the constant J is referred to as the Jellett's constant [13] and our numerical result indicates that this constant is zero throughout the precession process.

As a benchmark, we use our numerical scheme to show the behaviour of the classical macro scale tippe top with zero magnetic force. Here, the values of parameters are taken to be $R = 0.015$ m, $a = 0.1R$ m, $M = 0.015$ kg, $A = C = (2/5)MR^2$ and $\mu = 0.1$, with initial conditions: $\theta = 0.1$, $\omega = 100$, $\Omega = 0$ and $\dot{\mathbf{X}} = (0, 0, 0)$. Thus, from Eqs. (5) and (6) we obtain numerical results for nutation angle $\theta(t)$ as illustrated graphically in Fig. 7. From this figure, we can see that θ approaches π implying that the top flips over, which is consistent with Ueda *et al.* [13].

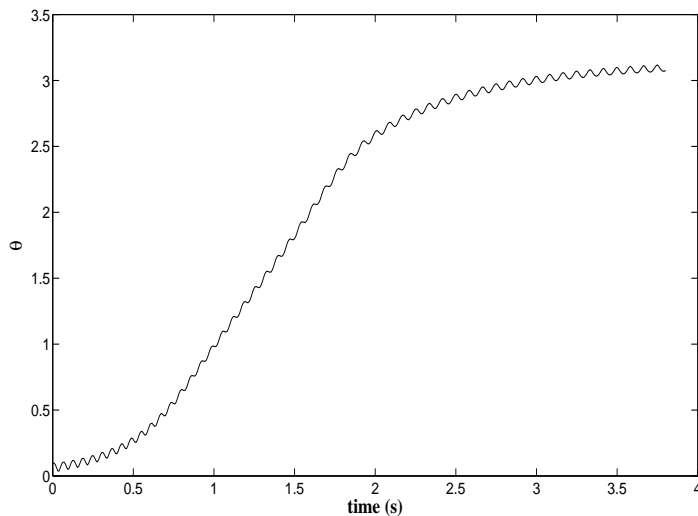


Figure 7: Nutation angle θ for classical macro scale tippe top

B Stability analysis

In this section, we use a simple stability argument to investigate the stability of the nano top for $\theta = 0$, $\pi/2$ and π . Without the external magnetic retarding force, i.e. $H_x = H_y = 0$, we consider a small perturbation around the standing up axis, namely $\theta = \epsilon$ for small $\epsilon > 0$. Eq. (4)₁ becomes

$$\ddot{\epsilon} = -aN\epsilon/A, \quad (11)$$

which implies that the spinning nano top is always stable. If we incorporate the external magnetic retarding force, i.e. $H_x = H_y = H$, which is a constant. For $\theta = \epsilon$, Eq. (4)₁ becomes

$$\ddot{\epsilon} = -aN\epsilon/A + (R - a)H/A, \quad (12)$$

which also implies that the nano top is stable. We note that for the case $\theta = \epsilon$, we assume $\Omega = 0$.

Next, we check the stability of the nano top at $\theta = \pi$. Upon substituting $\theta = \pi - \epsilon$, Eq. (4)₁ becomes

$$\ddot{\epsilon} = \frac{(C + A)\Omega^2 + aN}{A}\epsilon - \frac{(R + a)H}{A}, \quad (13)$$

noting that $\omega = \Omega$ when θ tends to π . Eq. (13) implies that the nano top is always unstable, and therefore it does not flip over.

For the lying down position, i.e. $\theta = \pi/2 - \epsilon$, Eq. (4)₁ becomes

$$\ddot{\epsilon} = -\frac{A\Omega^2 - aH}{A}\epsilon - \frac{HR - C\omega\Omega - aN}{A}, \quad (14)$$

which is stable if $A\Omega^2 - aH > 0$ or $\Omega^2 > aH/A$.

C Asymptotic expansion for $\theta = \pi/2$

In this section, we check the compatibility between our numerical results and the asymptotic expansions for the governing ordinary differential equations given in Eq. (2) or Eq. (4) when the nano top is lying down and the time t is sufficiently large. Upon substituting $\theta = \pi/2$ into Eqs. (4)₁, (4)₃, (5)₁ and (5)₂, we obtain

$$\begin{aligned} \Omega &= RH/(C\omega), \quad \dot{\omega} = -RH/C, \\ m\dot{u}_x &= m\Omega u_y - H, \quad m\dot{u}_y = -m\Omega u_x - H, \end{aligned} \quad (15)$$

respectively. Noting here that we assume $H_x = H_y = H$. From Eq. (15)₂, upon integrating both sides by t , we have

$$\omega = -Rht/C + c_1. \quad (16)$$

This asymptotic expansion and its corresponding numerical result for ω are plotted together in Fig. 8. We note that the constants used here are given by $R = 3.55 \text{ \AA}$, $C = 0.5A$, $A = (2/3)mR^2$, $m = 1.196 \times 10^{-24} \text{ kg}$ and $H = 0.1 \text{ zN}$. We fit Eq. (16) with the numerical solution for ω and obtain $c_1 = 3 \times 10^6$. Upon knowing ω , we can determine Ω by utilizing

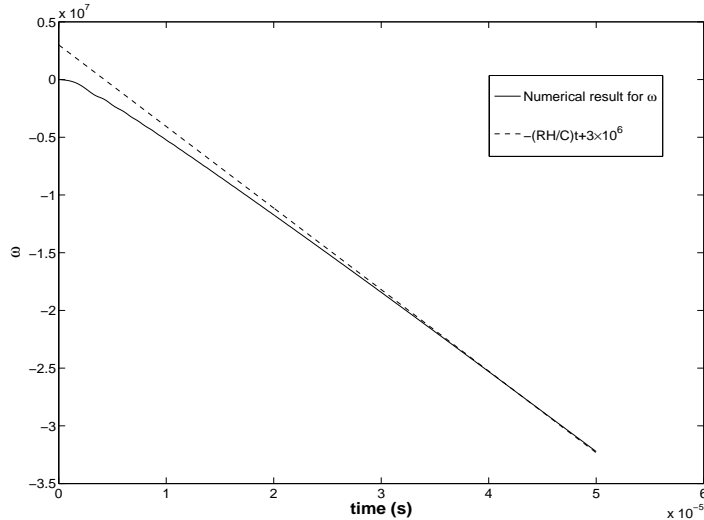


Figure 8: Asymptotic expansion for ω

Eq. (15)₁ as

$$\Omega = \frac{RH}{c_1 C - Rht}, \quad (17)$$

where this asymptotic equation decays to zero for a sufficiently large t and the corresponding result with its numerical solution are plotted in Fig. 9. Given the asymptotic

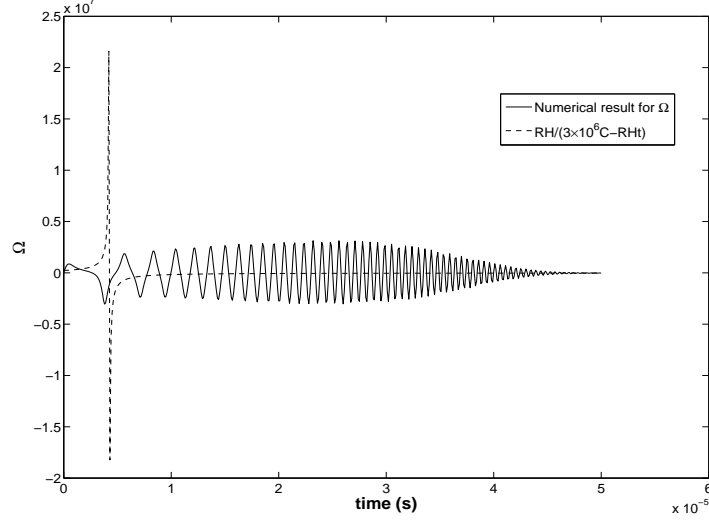


Figure 9: Asymptotic expansion for Ω

expansions for Ω , we can determine the asymptotic expansions for both u_x and u_y , which are given by

$$\begin{aligned} m\dot{u}_x &= \frac{mRH}{(c_1C - RHt)}u_y - H, \\ m\dot{u}_y &= -\frac{mRH}{(c_1C - RHt)}u_x - H. \end{aligned} \quad (18)$$

We can solve Eq. (18) analytically by introducing $v = u_x + iu_y$, where $i = \sqrt{-1}$. By multiplying i both sides of Eq. (18)₂ and combining with Eq. (18)₁ we have

$$\dot{v} + \frac{RH i}{(c_1C - RHt)}v = -\frac{H}{m}(1 + i). \quad (19)$$

By multiplying both sides of Eq. (19) by an integrating factor $\exp(-i \log(c_1C - RHt)) = 1/(c_1C - RHt)^i$ we obtain

$$\frac{d}{dt} \left(\frac{v}{(c_1C - RHt)^i} \right) = -\frac{H}{m} \frac{(1 + i)}{(c_1C - RHt)^i},$$

which on integrating we deduce

$$\frac{v}{(c_1C - RHt)^i} = \frac{(1 + i)}{(1 - i)} \frac{1}{Rm} (c_1C - RHt)^{1-i} + c_2,$$

where c_2 denotes a constant. Thus, the solution of Eq. (19) is given in the form

$$v(t) = \frac{(1 + i)}{(1 - i)} \frac{(c_1C - RHt)}{Rm} + c_2 e^{i \log(c_1C - RHt)}. \quad (20)$$

To determine the complex constant c_2 to fit our numerical data, we assign at $t = t^*$, $u_x(t^*) = u_1$ and $u_y(t^*) = u_2$, where u_1 and u_2 are constants. Thus, c_2 is given by

$$c_2 = e^{-i \log \lambda} \left\{ u_1 + iu_2 - \frac{i\lambda}{Rm} \right\},$$

where $\lambda = c_1 C - RHt^*$. Upon substituting into Eq. (20) and simplifying we have

$$v(t) = \frac{i(c_1 C - RHt)}{Rm} + e^{i\beta(t)} \left\{ u_1 + iu_2 - \frac{i\lambda}{Rm} \right\},$$

where $\beta(t) = \log([c_1 C - RHt]/\lambda)$. Next, we expand the above equation using Euler's formula, $e^{i\beta} = \cos \beta + i \sin \beta$, to obtain

$$\begin{aligned} v(t) = & u_1 \cos \beta(t) + \left\{ \frac{\lambda}{Rm} - u_2 \right\} \sin \beta(t) + \frac{i(c_1 C - RHt)}{Rm} \\ & + iu_1 \sin \beta(t) - i \left\{ \frac{\lambda}{Rm} - u_2 \right\} \cos \beta(t). \end{aligned} \quad (21)$$

Since $v = u_x + iu_y$, Eq. (21) gives rise to analytical solutions for u_x and u_y , namely

$$\begin{aligned} u_x = & u_1 \cos \beta(t) + \left\{ \frac{\lambda}{Rm} - u_2 \right\} \sin \beta(t), \\ u_y = & \frac{(c_1 C - RHt)}{Rm} + u_1 \sin \beta(t) - \left\{ \frac{\lambda}{Rm} - u_2 \right\} \cos \beta(t). \end{aligned} \quad (22)$$

The solutions (22) for u_x and u_y are plotted together with their corresponding numerical results in Figs. 10 and 11, respectively. We note that the values of constants used here are taken to be $t^* = 5 \times 10^{-5}$ s, $u_1 = -6 \times 10^{-7}$ ms⁻¹ and $u_2 = -4 \times 10^{-3}$ ms⁻¹. As can be seen from these figures, the solutions (22) agree with the numerical results for sufficiently large t .

D Retarding magnetic force as step function

In this section, we investigate the precession of the nano top subject to a magnetic force which is applied only in the y -direction and only for a finite time t_0 . In particular, we consider $H_y = HH(t_0 - t)$, where H is a constant representing the strength of the magnetic force, $H(t)$ is the Heaviside unit step function and t_0 denotes the time when the magnetic force is switched off. Two cases are examined, namely $t_0 = 0.8 \times 10^{-5}$ and 10^{-6} seconds. We observe that in the former case the nano top precesses from its initial standing up position to $\theta = 2.1$ soon after the retarding magnetic field is switched off and then it oscillates about $\theta = \pi/2$, as demonstrated in Fig. 12. The effect of the Heaviside function can be seen from the behaviour of ω , which is shown in Fig. 13. From this figure, before the switch off time $t_0 = 0.8 \times 10^{-5}$, the magnitude of ω increases but in the opposite direction with respect to the direction of the initial spin due mainly to the retarding magnetic force. After $t = 0.8 \times 10^{-5}$, since the retarding force is switched off, the magnitude of ω starts to decrease by the effect of the frictional force only. For the latter case, we find from Fig. 14 that the application of H_y for 10^{-6} s does not provide sufficient angular momentum for the nano top to lie down in a stable configuration. The variation of the corresponding ω for this case is presented in Fig. 15.

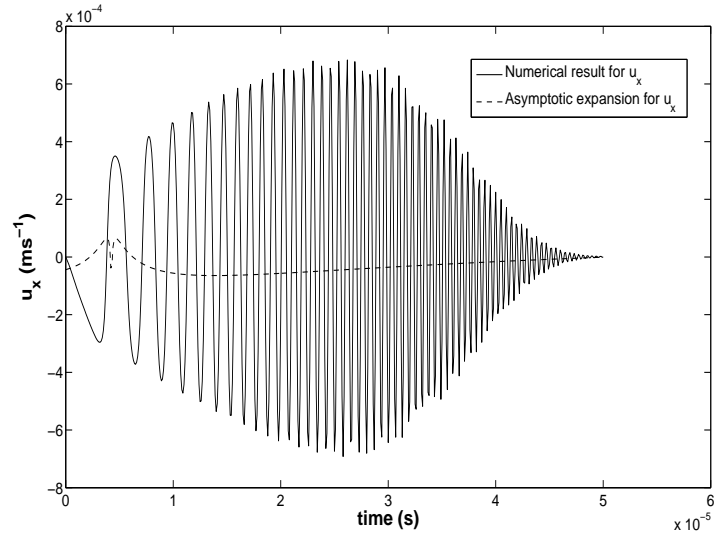


Figure 10: Asymptotic expansion for u_x $(22)_1$ in comparison with numerical result

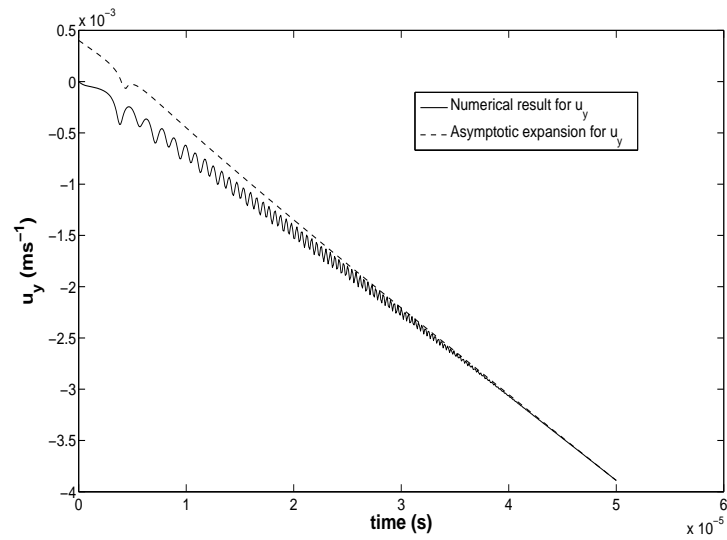


Figure 11: Asymptotic expansion for u_y $(22)_2$ in comparison with numerical result

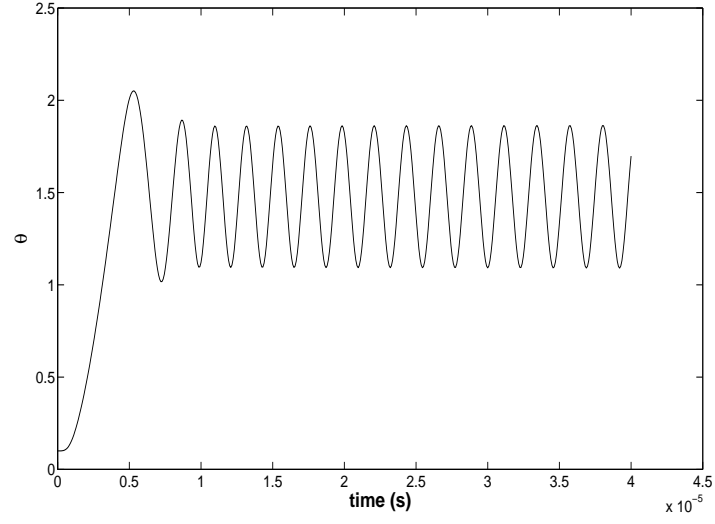


Figure 12: Nutation angle θ for nano top when $H_x = 0$ and $H_y = HH(t_0 - t)$ where $t_0 = 0.8 \times 10^{-5}$ s

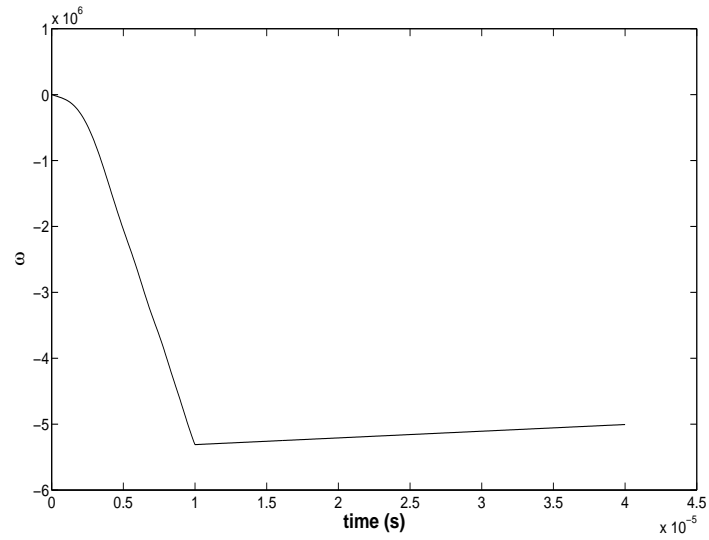


Figure 13: Angular frequency ω for nano top when $H_x = 0$ and $H_y = HH(t_0 - t)$ where $t_0 = 0.8 \times 10^{-5}$ s

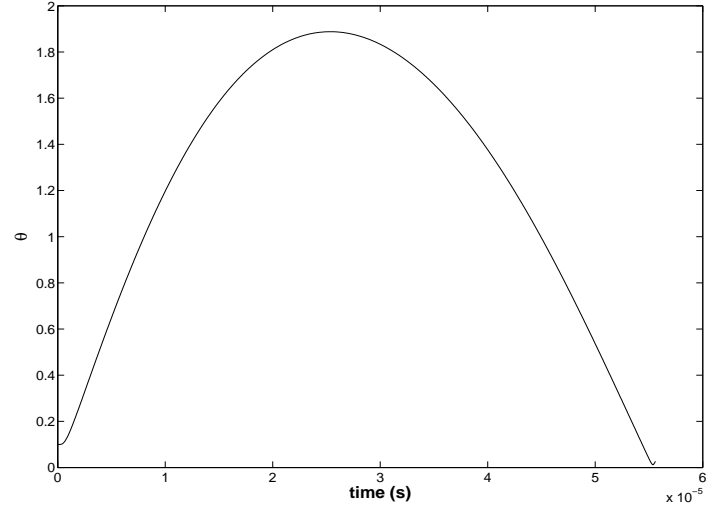


Figure 14: Nutation angle θ for nano top when $H_x = 0$ and $H_y = HH(t_0 - t)$ where $t_0 = 10^{-6}$ s

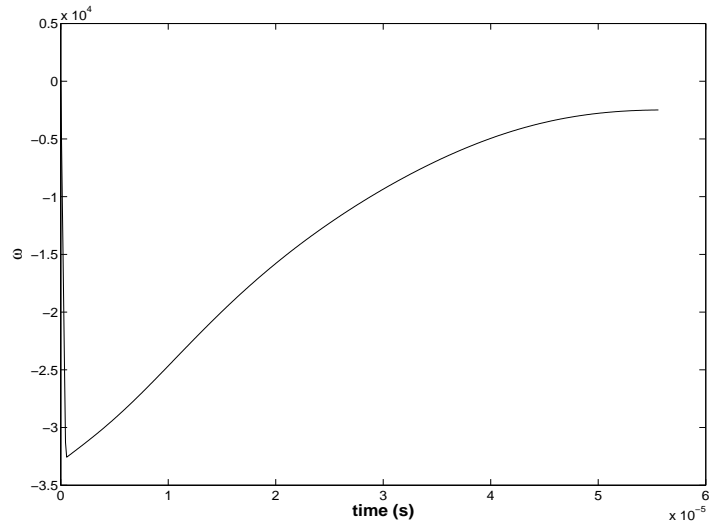


Figure 15: Angular frequency ω for nano top when $H_x = 0$ and $H_y = HH(t_0 - t)$ where $t_0 = 10^{-6}$ s

References

- [1] H. W. Kroto, J. R. Heath, S. C. O'Brien, R. F. Curl and R. E. Smalley, C_{60} : Buckminsterfullerene, *Nature* 318 (1985) 162.
- [2] S. Iijima, Helical microtubules of graphitic carbon, *Nature* 354 (1991) 56.
- [3] A. C. Or, The dynamics of a tippe top, *SIAM J. Appl. Math.* 54 (1994) 597-609.
- [4] H. Leutwyler, Why some tops tip, *European J. Phys.* 15 (1994) 59-61.
- [5] S. Ebenfeld and F. Scheck, A new analysis of the tippe top: Asymptotic states and Liapunov stability, *Ann. Physics* 243 (1995) 195-217.
- [6] C. G. Gray and B. G. Nickel, Constants of the motion for nonslipping tippe tops and other tops with round pegs, *Amer. J. Phys.* 68 (2000) 821-828.
- [7] N. M. Bou-Rabee, J. E. Marsden and L. A. Romero, Tippe top inversion as a dissipation-induced instability, *SIAM J. Appl. Dynam. Systems* 3 (2004) 352-377.
- [8] C. M. Braams, On the influence of friction on the motion of a top, *Physica* 18 (1952) 503-514.
- [9] N. M. Hugenholtz, On tops rising by friction, *Physica* 18 (1952) 515-527.
- [10] R. J. Cohen, The tippe top revisited, *Amer. J. Phys.* 45 (1977) 12.
- [11] A. G. Nasibulin, P. V. Pikhitsa, H. Jiang, D. P. Brown, A. V. Krashenninnikov, A. S. Anisimov, P. Queipo, A. Moisala, D. Gonzalez, G. Lientschnig, A. Hassanien, S. D. Shandakov, G. Lolli, D. E. Resasco, M. Choi, D. Tománek and E. I. Kauppinen, A novel hybrid carbon material, *Nature Nanotechnology* 2 (2006) 156-161.
- [12] D. Baowan, B. J. Cox and J. M. Hill, Discrete and continuous approximations for nanobuds, submitted for publication (2008).
- [13] T. Ueda, K. Sasaki and S. Watanabe, Motion of the tippe top: Gyroscopic balance condition and stability, *SIAM J. Appl. Dynam. Systems* 4 (2005) 1159-1194.
- [14] M. R. Falvo, R. M. Taylor, A. Helser, V. Chi, F. P. Brooks, S. Washburn and R. Superfine, Nanometre-scale rolling and sliding of carbon nanotubes, *Nature* 397 (1999) 236.
- [15] A. N. Kolmogorov and V. H. Crespi, Smoothest bearings: Interlayer sliding in multiwalled carbon nanotubes, *Phys. Rev. Lett.* 85 (2000) 4727.
- [16] H. K. Moffatt and Y. Shimomura, Spinning eggs - a paradox resolved, *Nature* 416 (2002) 385-386.
- [17] R. A. Wood, M. H. Lewis, M. R. Lees, S. M. Bennington, M. G. Cain and N. Kitamura, Ferromagnetic fullerene, *J. Phys.: Condens. Matter* 14 (2002) L385-L391.
- [18] G. V. Dedkov and A. A. Khasov, Electromagnetic friction forces on the scanning probe asperity moving near surface, *Phys. Lett. A* 259 (1999) 38-42.

- [19] G. V. Dedkov, Friction on the nanoscale: New physical mechanisms, *Mater. Lett.* 38 (1999) 360-366.
- [20] F. Family, H. G. E. Hentschel and Y. Braiman, Friction at the Nanoscale, *J. Phys. Chem. B* 104 (2000) 3984-3987.
- [21] J. Servantie and P. Gaspard, Translational dynamics and friction in double-walled carbon nanotubes, *Phys. Rev. B* 73 (2006) 125428.
- [22] S. J. Heo and S. B. Sinnott, Effect of molecular interactions on carbon nanotube friction, *J. Appl. Phys.* 102 (2007) 064307.
- [23] R. L. Burden and J. D. Faires, *Numerical Analysis* (Thomson, South Bank, 2005) p. 313-322.